corrosion and materials degradation

MDPI

Article

Event-Based Evaluation of Short-Term Wettability Degradation of RTV Nanocomposite-Coated 150 kV Ceramic Insulators Under Tropical Flashover Stress

Yusreni Warmi [1,*], Nofriady Handra [2], Agus Sukarto Wismogroho [3], Syukri Syukri [4], Sitti Amalia [1], Andi M. Nur Putra [1], Hamdi Habdillah [5,6], Martini Martini [1] and Muhammad Naufalun Nabil [7]

1 Department of Electrical Engineering, Faculty of Engineering, Institut Teknologi Padang (ITP), Padang 25143, Indonesia; sittiamalia@itp.ac.id (S.A.); andimnurputra@itp.ac.id (A.M.N.P.); 202131006.martini@itp.ac.id (M.M.)
2 Department of Mechanical Engineering, Faculty of Engineering, Institut Teknologi Padang (ITP), Padang 25143, Indonesia; nofriady.h@itp.ac.id
3 National Research and Innovation Agency (BRIN), Kawasan Sains dan Teknologi (KST) B.J. Habibie, Serpong, South Tangerang 15314, Indonesia; agussukarto@gmail.com
4 Department of Chemistry, Faculty of Mathematics and Natural Sciences, Universitas Andalas (UNAND), Padang 25163, Indonesia
5 Division of Information and Communication Technology (BITKOM), Institut Teknologi Padang (ITP), Padang 25143, Indonesia; hamdi@itp.ac.id
6 Faculty of Computing, Universiti Teknologi Malaysia (UTM), Johor Bahru 81310, Malaysia
7 Department of Mechanical Engineering, Faculty of Engineering, Universitas Andalas (UNAND), Padang 25163, Indonesia; mnaufalunnabil@gmail.com
* Correspondence: yusreni@itp.ac.id; Tel.: +62-813-6344-4072

Abstract

Flashover events can induce rapid surface condition changes on outdoor ceramic insulators, while early-stage degradation is typically assessed indirectly through long-term ageing or electrical diagnostics. This study proposes an event-based, surface-focused evaluation framework to assess short-term flashover-induced surface degradation using normalized wettability indicators. A controlled experimental comparison was conducted on uncoated, TiO_2-RTV-coated, and SiO_2-RTV-coated 150 kV ceramic insulators subjected to a single flashover pre-stress under humid tropical conditions. Static contact angles decreased from 42.6° to 18.3° for uncoated ceramic, from 112.4° to 86.7° for TiO_2-RTV, and from 115.8° to 92.6° for SiO_2-RTV after flashover exposure. The corresponding relative wettability retention values were 43.0%, 77.1%, and 80.0%, while the wettability degradation index values were 0.57, 0.23, and 0.20, respectively. Surface morphology and elemental presence were qualitatively examined via SEM–EDS. The results show that both nanocomposite coatings effectively preserve post-flashover surface hydrophobicity compared with uncoated ceramics, with the SiO_2-RTV system exhibiting the highest short-term wettability retention. By integrating static contact-angle measurements, qualitative surface morphology, and normalized wettability indicators, this study proposes an event-based evaluation framework for RTV-coated ceramic insulators. Flashover-voltage and leakage-current measurements were included only as supplementary validation to support the surface-based interpretation, without implying direct electrical performance modeling. This surface-focused, event-based approach provides an experimental basis for post-flashover condition assessment of ceramic insulators operating in humid outdoor environments.

Check for updates

Academic Editor: Raman Singh

Received: 5 February 2026
Revised: 19 March 2026
Accepted: 27 March 2026
Published: 30 March 2026

Copyright: © 2026 by the authors. Licensee MDPI, Basel, Switzerland. This article is an open access article distributed under the terms and conditions of the Creative Commons Attribution (CC BY) license.

Keywords: ceramic insulator; RTV nanocomposite coating; flashover stress; short-term wettability degradation; surface hydrophobicity; event-based evaluation

1. Introduction

Ceramic insulators operating in humid tropical environments are highly susceptible to moisture-assisted surface conduction and discharge activity, which can accelerate contamination processes and reduce surface resistance under wet operating conditions [1–7]. To mitigate these effects, room-temperature-vulcanized (RTV) silicone coatings have been widely applied because of their inherent hydrophobicity and their ability to suppress continuous water-film formation on ceramic surfaces in polluted and high-humidity environments [8–13].

Recent studies have investigated the incorporation of TiO_2 and SiO_2 nanoparticles into RTV matrices to improve surface wettability, hydrophobic stability, and resistance to moisture-assisted surface conduction in outdoor insulation systems [14–17]. However, most published studies primarily emphasize contact-angle enhancement, pollution flashover performance, or long-term ageing behavior [18–20]. Only limited attention has been given to the immediate post-event surface condition following a controlled flashover exposure, particularly under humid tropical conditions. In addition, many reports discuss filler–matrix mechanisms beyond what can be directly supported by contact-angle data, SEM images, or EDS spectra alone. Accordingly, the present study defines its scope more narrowly and avoids mechanistic claims that are not directly supported by the experimental dataset.

The present study provides a controlled comparison of uncoated, TiO_2-RTV-coated, and SiO_2-RTV-coated 150 kV ceramic surfaces by quantifying static contact angles before and after controlled flashover exposure under high-humidity tropical conditions and by qualitatively examining surface morphology and elemental presence using SEM–EDS. The discussion is intentionally limited to observable wettability changes and qualitative surface features, whereas mechanistic chemical interpretations and long-term degradation behavior are deliberately excluded because of the scope and nature of the experimental dataset.

Unlike previous studies that primarily emphasize long-term electrical performance or mechanistic interpretation, this work provides a controlled short-term comparative assessment of TiO_2-RTV and SiO_2-RTV nanocomposite coatings applied to 150 kV ceramic insulators under tropical flashover pre-stress. The novelty of this study lies in the following:

(1) the use of a single, controlled flashover event as a surface pre-conditioning step;

(2) the direct comparison of post-flashover wettability retention between TiO_2-RTV and SiO_2-RTV coatings under identical environmental conditions; and

(3) the strictly qualitative interpretation of surface morphology and elemental presence without invoking unmeasured electrical or chemical mechanisms. This approach provides focused experimental insight into the short-term surface degradation behavior of RTV-based coatings relevant to humid tropical environments.

In addition to electrical insulation reliability, surface wettability is closely associated with moisture-driven surface degradation processes because it governs moisture retention, thin electrolyte-film formation, and contaminant ion accumulation on exposed ceramic surfaces [1–3]. Hydrophilic or poorly stabilized surfaces facilitate persistent water layers that act as conductive electrolytes, thereby promoting ionic transport and progressive surface deterioration under humid or polluted environments [4–10]. In this context, wettability behavior is not merely a surface property, but a key controlling factor in moisture-assisted

degradation pathways that precede persistent electrolyte-film formation and long-term ageing phenomena.

From the perspective of surface degradation and environmental ageing, the present study focuses on early-stage surface stabilization by correlating coating morphology, qualitative surface condition, and wettability response. Rather than directly quantifying long-term material deterioration, this work emphasizes the initial surface condition that governs moisture retention and electrolyte-film persistence, both of which are recognized as critical precursors to moisture-driven surface degradation. This surface-focused approach provides an experimental basis for comparing early-stage surface degradation behavior without extending the interpretation beyond the measured evidence.

In outdoor high-voltage insulation systems, surface wettability plays a critical role in governing moisture retention and water-film continuity, which directly influence moisture-driven surface degradation processes. Under humid and contaminated conditions, increased wettability promotes sustained moisture residence on ceramic insulator surfaces, accelerating degradation pathways that can lead to persistent electrolyte-film formation and progressive surface deterioration. Therefore, evaluating wettability behavior provides a surface-sensitive indicator for assessing early-stage degradation mechanisms relevant to moisture-driven surface deterioration in outdoor insulation environments.

2. Materials and Methods

2.1. Material

Ceramic insulator segments (porcelain, 150 kV class) were obtained from the Indonesian transmission network operator PLN-P3BS and used as test substrates representative of field-installed line insulators [2,6]. The base coating matrix was a commercial room-temperature-vulcanized (RTV) silicone rubber (Dow Corning 3140, Dow Corning Corporation, Midland, MI, USA), which has been widely adopted for outdoor insulation applications because of its hydrophobic surface properties and environmental stability [9,18,19].

Two nanofiller systems were selected based on previously reported RTV nanocomposite formulations for high-voltage insulation: TiO_2 nanoparticles (anatase phase, average size 20–30 nm) and SiO_2 nanoparticles (amorphous, average size 15–25 nm) [8,16,21–23]. The nanoparticle loading was fixed at 2 wt.% relative to the RTV matrix, consistent with concentrations reported to improve hydrophobic behavior without excessively increasing viscosity or compromising coating integrity [8,16,17,21]. A silane coupling agent and a silicone-based surfactant supplied with the RTV kit were used to aid dispersion and adhesion; however, their detailed compositions were not disclosed by the manufacturer. Consequently, the present study interprets coating behavior strictly in terms of observable physical properties (contact angle and surface morphology) without inferring specific chemical interactions between nanofillers and the RTV matrix [16–18].

All raw materials were stored at 25 ± 2 °C and 50–60% relative humidity prior to use, following standard handling recommendations for RTV-based outdoor insulation systems [9,24].

2.2. Preparation of TiO_2-RTV and SiO_2-RTV Nanocomposite Coatings

The nanocomposite mixtures were prepared by ultrasonication for 30 min to disperse the TiO_2 or SiO_2 nanoparticles, followed by mechanical stirring for homogenization. Coatings were applied using a controlled spray-deposition method, selected for reproducibility and surface uniformity. The coated specimens were then allowed to cure under ambient humidity for 24 h.

To improve clarity, the complete experimental workflow is illustrated in Figure 1.

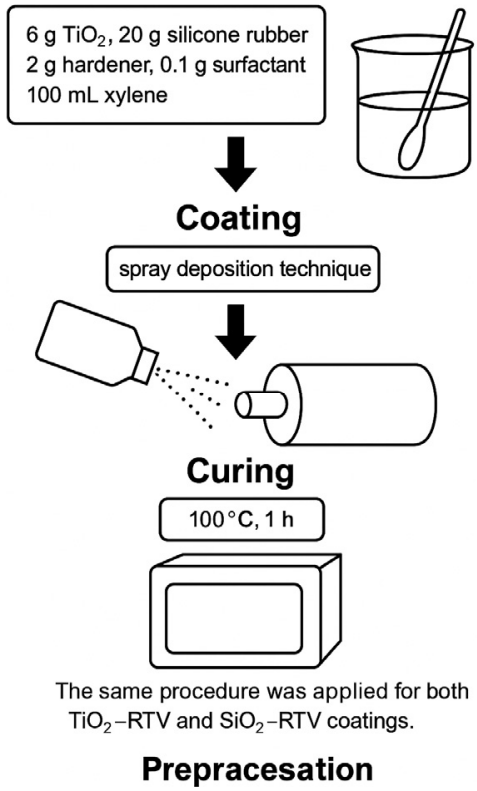


Figure 1. Experimental workflow for coating preparation, application, curing, flashover exposure, and post-flashover characterization procedures used in this study. The arrow indicates the spray-deposition step used to apply the TiO_2-RTV and SiO_2-RTV coatings onto the ceramic substrate before curing.

2.3. Coating Preparation and Application

The RTV-based composite coatings were prepared by dispersing TiO_2 or SiO_2 nanoparticles into a room-temperature-vulcanized silicone rubber matrix using ultrasonication for 30 min, followed by mechanical stirring to obtain a homogeneous suspension, following procedures commonly adopted for nanoparticle-modified RTV coatings applied to high-voltage ceramic insulators [14–17]. The nanoparticle content and mixing procedure were kept identical for all coated specimens to ensure consistency between samples. Prior to coating application, the ceramic insulator surfaces were cleaned using sequential rinsing with deionized water and ethanol, followed by air drying at ambient conditions to remove surface contaminants, as recommended in previous studies on surface conditioning for RTV-coated ceramic substrates [8–13].

The prepared RTV composite was applied uniformly onto the ceramic surfaces using a controlled spray-coating technique. Key deposition parameters, including spray distance, application angle, number of coating passes, and curing conditions, were maintained consistently for all specimens to minimize variability in coating morphology and surface coverage [10,11,19]. After application, the coated samples were cured for 24 h at ambient laboratory conditions (25 ± 2 °C; 50–60% relative humidity) before subsequent tropical-humidity preconditioning.

Coating thickness was not quantified using magnetic or eddy-current measurement instruments, as such techniques are not applicable to non-conductive ceramic substrates. Instead, coating uniformity and surface coverage were ensured through controlled deposition parameters and visual inspection to confirm the formation of a continuous RTV layer across the ceramic surface, consistent with qualitative thickness-control approaches reported in related RTV coating studies [16,19].

2.4. Sample Grouping and Preconditioning

Three sample groups were prepared for comparative evaluation: uncoated ceramic insulators (control), ceramic insulators coated with TiO_2-RTV nanocomposite, and ceramic insulators coated with SiO_2-RTV nanocomposite.

Each group comprised $n = 3$ specimens, which is consistent with sample sizes typically used in hydrophobicity and surface characterization studies of RTV-coated insulators [8,25].

After curing, all specimens were placed in a climate chamber and preconditioned at 28–33 °C and 80–90% relative humidity for seven days to simulate tropical moisture exposure conditions prior to flashover testing. Similar temperature and humidity ranges have been reported to accelerate surface wetting and contamination effects on outdoor insulators in tropical environments [6,7]. This preconditioning step ensured that all coated and uncoated samples reached a comparable initial moisture-adsorption state, in line with recommendations for comparative evaluation of insulator surface performance under humid conditions [8,11,25].

2.5. Flashover Exposure Under Tropical Conditions

The flashover pre-stress experiment was performed to simulate a short-term electrical surface-disturbance event under humid tropical conditions. Each specimen was exposed to a single controlled flashover event prior to post-test surface evaluation. The purpose of this stage was not to establish a predictive breakdown model, but to generate a reproducible electrical pre-stress condition for subsequent assessment of wettability change and surface morphology response [11,26].

In accordance with the experimental scope, predictive flashover modeling was not attempted. The flashover stage in this study primarily served as a controlled electrical pre-stress step for subsequent hydrophobicity and surface morphology assessments, while flashover-voltage and leakage-current measurements were included only as supplementary validation of the surface-based interpretation [11,26]. Thus, the main role of the flashover experiment was to create a consistent post-stress surface condition for comparative evaluation among the uncoated, TiO_2-RTV-coated, and SiO_2-RTV-coated ceramic insulators under the investigated humid-environment scenario.

2.6. Contact-Angle Measurement

Static water contact angles were measured using a goniometer (Ossila L2004A1, Ossila Ltd., Sheffield, UK) with a 5 μL droplet volume. Three measurements were taken at different positions on each specimen, and the mean value was reported. Measurements were performed before and after flashover exposure to evaluate changes in surface wettability as an indicator of short-term surface-condition degradation, following standard RTV hydrophobicity procedures [18,26,27].

Surface morphology and elemental composition were qualitatively examined using scanning electron microscopy coupled with energy-dispersive spectroscopy (SEM-EDS) to identify post-stress surface features and coating continuity characteristics [8,11,28]. The primary analytical focus of the present study was placed on surface wettability and qualitative surface characterization, while flashover-voltage and leakage-current measurements were used only as supplementary validation rather than as the principal diagnostic basis [11,26]. Accordingly, the integrated interpretation of coating performance was established mainly from contact-angle behavior, qualitative surface morphology, and normalized wettability indicators, with the electrical measurements used to support the consistency of the surface-based evaluation. During acquisition, each droplet profile was visually checked to ensure a stable baseline and a clearly distinguishable contour before the contact angle was recorded. A representative measurement setup is provided in Figure 2. In response to the reviewer's

request, representative raw contact-angle captures obtained from the goniometer software are now additionally provided in Appendix A to show the droplet profile, baseline fitting, and left/right angle detection used during measurement. The comparative analysis and statistical discussion in the main text remain based on the averaged contact-angle values obtained from three measurement positions on each specimen.

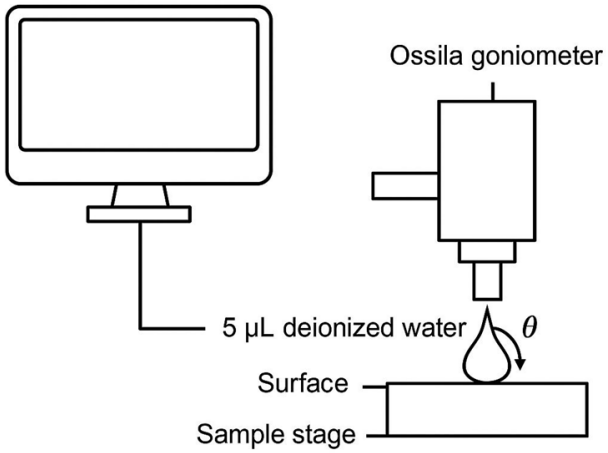


Figure 2. Contact-angle measurement setup.

2.7. SEM-EDS Surface Characterization

Surface morphology was observed using a JEOL JSM-6510LV scanning electron microscope (JEOL Ltd., Tokyo, Japan), and elemental composition was analyzed via energy-dispersive spectroscopy (EDS). SEM analyses were qualitative only and limited to identifying surface features such as cracks, roughness, or particle distribution. EDS analysis was used solely to confirm elemental presence (Si, Ti, O), without interpreting chemical bonding or reaction behavior [8,27]. For clearer presentation, the EDS spectra are shown as processed figure outputs with labeled elemental peaks while preserving the original analytical trend recorded by the instrument. Within the scope of this study, the EDS discussion is limited to qualitative elemental confirmation and comparative peak-intensity observation relevant to surface-condition changes before and after flashover exposure; accordingly, elemental percentage values are not reported.

2.8. Coating Thickness Control

The coating application process was standardized by controlling the RTV formulation viscosity, spray distance, number of coating passes, and curing conditions for all specimens. Because magnetic and eddy-current thickness gauges are not applicable to non-conductive ceramic substrates, no direct thickness values obtained using such instruments are reported. Coating uniformity was ensured through controlled deposition parameters and visual verification of continuous surface coverage across the ceramic insulator surface. This qualitative approach to thickness control is appropriate for preliminary surface-property studies on non-conductive ceramic substrates, where thickness uniformity is maintained through controlled deposition parameters rather than direct instrumental measurement.

2.9. Statistical Analysis

One-way ANOVA with $\alpha = 0.05$ was used to determine statistical differences between groups. Tukey posthoc tests were applied when significant differences were detected. Statistical analysis was performed in OriginPro 2023. No regression modeling, mechanistic correlation, or predictive analysis was conducted [20]. Because each group comprised $n = 3$ specimens, the statistical results are interpreted as preliminary comparative evidence under controlled laboratory conditions rather than population-level estimates.

2.10. Summary of the Experimental Procedure

Coating thickness-control procedures and statistical analysis were applied to improve data consistency across all sample groups. To enhance coating comparability, controlled deposition parameters, including spray distance, spray angle, number of coating passes, and curing duration, were maintained consistently for all coated specimens [11,24]. Because the ceramic substrate was non-conductive, direct thickness measurement using magnetic or eddy-current gauges was not applicable. In addition, indirect thickness-estimation methods such as weight gain or cross-sectional microscopy were not applied in the present study. Therefore, coating comparability was ensured through controlled deposition conditions and visual verification of continuous and homogeneous surface coverage, rather than through absolute thickness quantification [11,26]. Statistical analysis was then applied to evaluate the consistency of the measured wettability parameters and the comparative surface-performance trends among the uncoated, TiO_2-RTV-coated, and SiO_2-RTV-coated insulator groups.

3. Results and Discussion

The observed changes in surface wettability following flashover exposure reflect alterations in moisture–surface interactions that are closely associated with moisture-driven surface degradation mechanisms. Reduced contact-angle stability indicates enhanced moisture retention on the ceramic surface, facilitating physicochemical surface processes that contribute to surface deterioration under humid conditions. From a surface-degradation perspective, wettability evolution serves as an indirect yet sensitive marker of surface-condition degradation, linking flashover-induced surface modification to persistent electrolyte-film formation and moisture-assisted surface conductivity under tropical environmental stress.

3.1. Hydrophobicity Enhancement

Contact-angle measurements demonstrate a clear improvement in surface hydrophobicity following the application of TiO_2-RTV and SiO_2-RTV nanocomposite coatings. The uncoated ceramic surface exhibits hydrophilic behavior, with contact-angle values ranging from 62° to 70°, which is consistent with previously reported characteristics of unprotected ceramic insulators exposed to humid tropical environments. Such hydrophilic behavior increases surface susceptibility to moisture accumulation under wet conditions, facilitating the formation of continuous surface water films along the insulator surface [6,12].

After coating application, both nanocomposite systems exhibit a distinct transition to hydrophobic surface behavior. The TiO_2-RTVcoated samples achieve an average contact angle of $105° \pm 3°$, while the SiO_2-RTV-coated samples show slightly higher values of $110° \pm 2°$. The relatively narrow standard deviations indicate consistent surface modification across all prepared specimens, suggesting uniform coating coverage and stable short-term wettability enhancement [27,28].

Following flashover exposure, hydrophobicity remains above 95° for both coated systems, whereas the uncoated ceramic surface experiences a pronounced reduction in contact angle. This post-flashover hydrophobic retention reflects reduced surface wettability under humid conditions rather than any form of performance enhancement beyond surface-related behavior. The observed trends are consistent with previous studies reporting improved moisture-shedding characteristics of RTV-based coatings and additive-assisted surface enhancement on ceramic and porcelain insulators in high-humidity environments [7,20,23,29].

Figure 3 presents the statistical distribution of contact-angle measurements obtained before and after flashover exposure. Although all samples experience some degree of

contact-angle reduction following flashover, the decline is most pronounced for the uncoated ceramic surface. Among the coated specimens, the SiO_2-RTV system retains the highest post-flashover contact-angle values, followed by the TiO_2-RTV system. These differences reflect variations in short-term surface wettability and are consistent with the qualitative surface features observed in subsequent SEM micrographs (Figures 4 and 5), without implying predictive behavior beyond the measured surface properties.

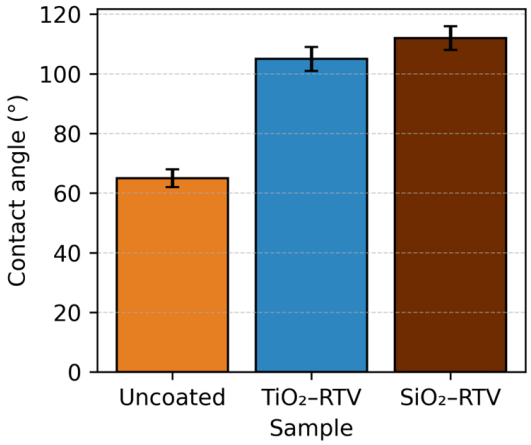


Figure 3. Mean static contact angle of uncoated, TiO_2-RTV, and SiO_2-RTV ceramic insulators measured before and after flashover exposure. Error bars represent ± standard deviation (n = 3).

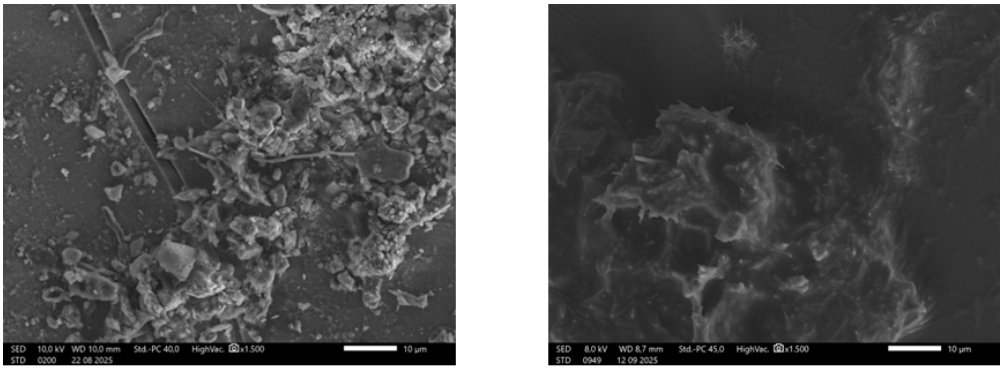


Figure 4. SEM micrographs of the TiO_2-RTV-coated ceramic surface: (**a**) before flashover exposure; (**b**) after flashover exposure (5000×).

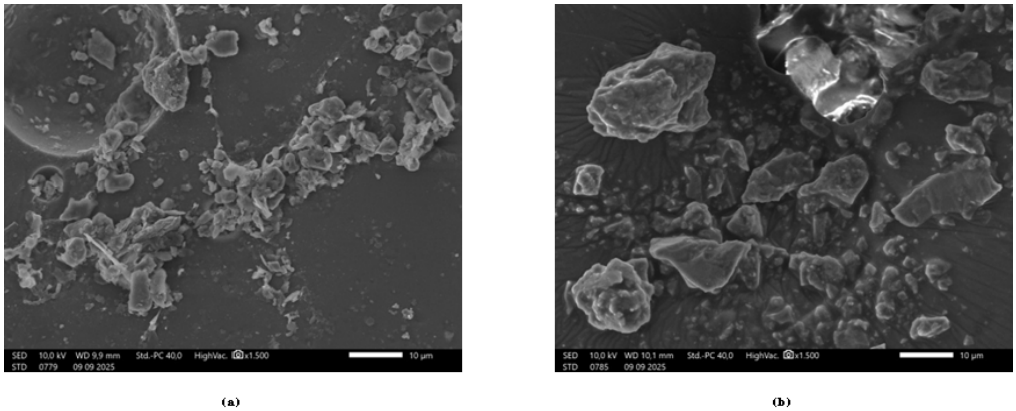


Figure 5. SEM micrographs of the SiO_2-RTV-coated ceramic surface: (**a**) before flashover exposure; (**b**) after flashover exposure (5000×).

Overall, the contact-angle results confirm that both TiO_2-RTV and SiO_2-RTV nanocomposite coatings provide measurable enhancement in short-term surface hydrophobicity relative to uncoated ceramic insulators. The findings presented in this section are limited to observable wettability behavior under the controlled tropical flashover conditions employed in this study and do not extend to long-term aging, durability, or mechanistic interpretations.

3.2. Surface Morphology and Elemental Distribution

Figures 4–6 provide experimental evidence that a single controlled flashover event induces distinct surface-condition states on ceramic insulators, depending on the presence and type of RTV-based nanocomposite coating. In this study, SEM–EDS is employed not as a microstructural characterization tool, but as a qualitative diagnostic method to identify post-flashover surface-condition differentiation relevant to wettability behavior under humid tropical environments.

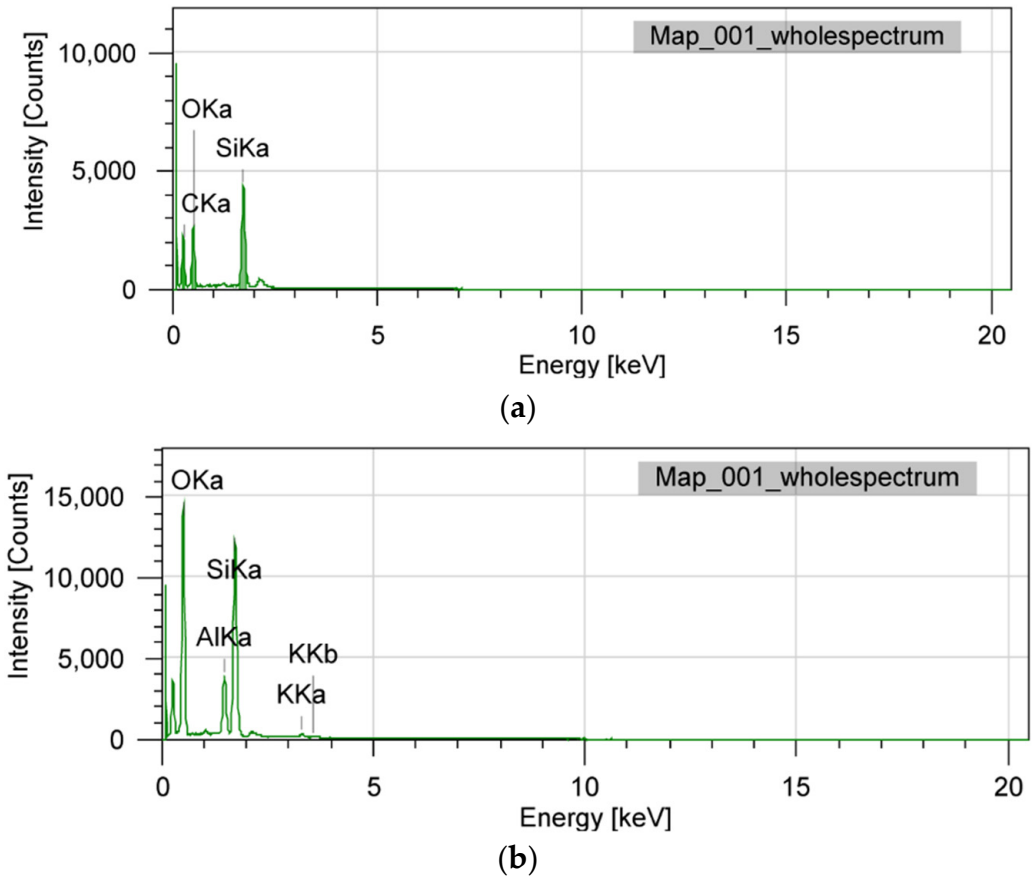


Figure 6. EDS spectra of the TiO_2-RTV-coated ceramic surface (**a**) before and (**b**) after flashover exposure, with the main detected elemental peaks identified for qualitative comparison.

As shown in Figure 4, the TiO_2-RTV-coated surface retains a largely continuous polymeric layer after flashover exposure. The SEM micrographs reveal limited development of open pores or interconnected microcracks, indicating that the RTV matrix remains structurally intact following electrical pre-stress. Although localized surface irregularities are visible at higher magnification, these features do not expose the underlying ceramic substrate. From a surface-condition perspective, this morphology suggests a reduced density of preferential moisture-adsorption sites, which is consistent with previously reported suppression of continuous water-film formation on RTV-coated insulators operating under humid conditions [7,20,24,27].

In contrast, Figure 5 shows that the SiO_2-RTV-coated surface exhibits an even more uniform post-flashover morphology, with fewer observable surface discontinuities compared with the TiO_2-RTV system. The smoother and more homogeneous surface texture indicates enhanced resistance of the coating layer to flashover-induced electro-thermal stress. This morphological stability provides experimental support for the higher post-flashover wettability retention observed for the SiO_2-RTV coating (Section 3.3), establishing a direct link between surface continuity and short-term hydrophobic stability under humid conditions. Similar correlations between surface smoothness and improved moisture repellency have been reported for silica-modified RTV coatings in polluted and high-humidity environments [16,20,30,31].

By contrast, the uncoated ceramic surface exhibits pronounced surface heterogeneity after flashover exposure, including open pores, microcracks, and heterogeneous deposits. Such features are widely recognized as surface-condition indicators associated with enhanced moisture adsorption and the formation of continuous surface water films, which precede leakage-current development and secondary discharge activity under humid conditions [6,12,20,32]. The absence of a protective polymeric layer allows flashover-induced stress to directly impact the ceramic substrate, resulting in irreversible surface-condition degradation.

The elemental information provided in Figure 6 further supports this surface-condition differentiation. The EDS spectra confirm the presence of Si and O associated with the RTV silicone matrix and Ti associated with the TiO_2 nanofiller, both before and after flashover exposure. Following flashover, increased C- and O-related signals are detected, which are attributed to discharge-related residues and environmental contamination rather than chemical modification or degradation of the coating material [20,30]. Importantly, no abrupt reduction or disappearance of coating-related elemental signals is observed, indicating that the coating layer remains present and continuous after flashover exposure. Consistent with the intrinsic limitations of EDS analysis, these results are interpreted solely as confirmation of elemental presence and not as evidence of uniform nanoparticle dispersion or chemical interaction [7,17,33,34].

Taken together, the SEM–EDS results demonstrate that flashover pre-stress produces three experimentally distinguishable surface-condition states:

(i) severe surface disruption and moisture-susceptible morphology on uncoated ceramic surfaces;
(ii) partially preserved surface continuity on TiO_2-RTV-coated surfaces; and
(iii) the most stable and uniform surface condition on SiO_2-RTV-coated surfaces.

This differentiation is experimentally significant because it provides a physical surface-condition basis for interpreting the wettability degradation trends discussed in Sections 3.3 and 3.4, without invoking unmeasured electrical performance or chemical degradation mechanisms.

The novelty of this section lies in repositioning SEM–EDS from serving as a descriptive imaging technique to a surface-condition diagnostic framework for short-term flashover assessment. Unlike previous studies that emphasize long-term aging, electrical flashover voltage, or mechanistic filler–matrix interactions [13,20], the present work demonstrates that early-stage flashover-induced surface-condition differentiation can be experimentally identified through qualitative surface continuity analysis and directly correlated with wettability retention metrics. This surface-focused diagnostic approach provides practical relevance for post-event condition assessment of ceramic insulators operating in humid tropical environments, where rapid identification of surface vulnerability is critical.

3.3. Wettability Response as an Experimental Signature of Post-Flashover Surface Condition

The wettability response quantified through static contact-angle measurements provides direct experimental evidence of flashover-induced surface-condition differentiation. Figures 7 and 8 present the contact-angle values measured before and after flashover exposure, emphasizing that the observed trends originate from experimentally measurable surface behavior rather than qualitative visual interpretation.

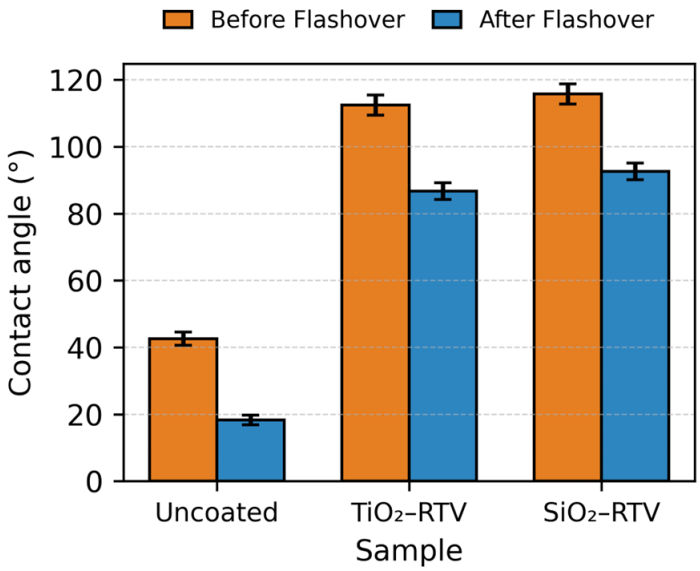


Figure 7. Static contact angle response before and after flashover pre-stress.

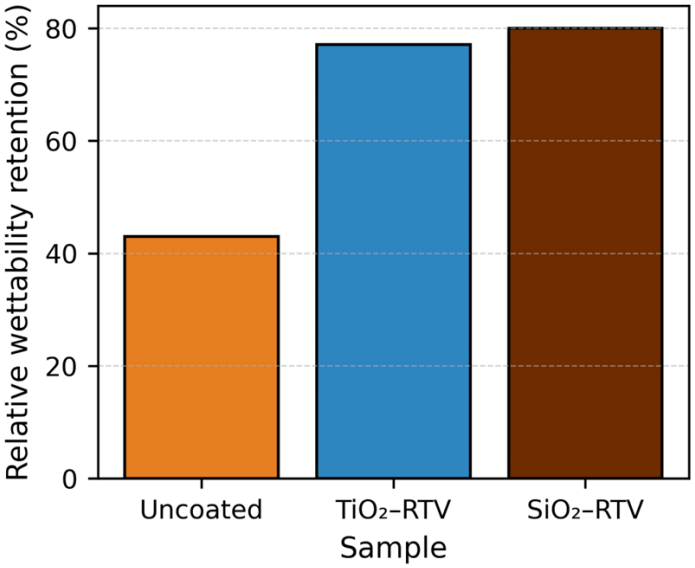


Figure 8. Relative wettability retention derived from static contact-angle measurements after flashover pre-stress.

As shown in Figure 7, the uncoated ceramic surface undergoes a pronounced reduction in static contact angle following flashover pre-stress. This abrupt wettability collapse signifies a rapid transition toward moisture continuity on the ceramic surface. From an experimental perspective, such a transition represents a critical surface-condition shift, as continuous water-film formation on ceramic insulators is widely recognized as an early-stage precursor to leakage-current escalation and surface discharge activity under humid operating conditions [6,12,20,32]. The magnitude of contact-angle reduction observed here

reflects irreversible surface-condition deterioration, consistent with the extensive surface disruption and pore exposure identified in SEM observations (Section 3.2).

In contrast, the TiO_2-RTV- and SiO_2-RTV-coated samples retain substantially higher post-flashover contact-angle values, as illustrated in Figure 7. This retained hydrophobicity experimentally confirms that the RTV-based coatings preserve the ability to disrupt continuous water-film formation even after electrical surface stressing. From a surface-condition standpoint, this behavior indicates delayed progression toward moisture-assisted conduction pathways, in agreement with previous studies on RTV-coated insulators subjected to humid and contaminated environments [7,20,24,27].

A more explicit comparison of short-term wettability stability is provided in Figure 8, which highlights the relative retention of post-flashover contact angles among the tested surfaces. The consistently higher retained contact-angle values for the coated samples demonstrate that surface protection fundamentally alters the post-flashover wettability response. Notably, the SiO_2-RTV coating exhibits the highest wettability retention, indicating the superior short-term stability of surface hydrophobicity under combined electrical and humid stress. Although the absolute difference between the two coating systems is moderate, its reproducibility across all specimens indicates that filler type influences early-stage surface-condition resilience rather than long-term material performance [16,20,30,31].

Importantly, the wettability response presented in Figures 7 and 8 is interpreted here not as an intrinsic material property but as an experimental signature of post-flashover surface condition. When evaluated alongside SEMEDS evidence (Section 3.2), the contact-angle results establish a coherent experimental framework linking flashover-induced surface disruption, surface continuity, and short-term moisture interaction. This integrated interpretation advances wettability measurements beyond descriptive hydrophobicity reporting and positions them as a surface-condition diagnostic indicator for early-stage assessment following flashover events.

The novelty of this section lies in the experimental use of post-flashover wettability response as a diagnostic marker of short-term surface-condition change. Unlike conventional studies that employ contact-angle measurements primarily to describe material hydrophobicity or long-term aging behavior [13,20], the present work demonstrates that contact-angle retention immediately after flashover exposure can differentiate degradation states of coated and uncoated ceramic insulators under tropical humidity. By explicitly correlating wettability trends (Figures 7 and 8) with surface-condition evidence from SEM-EDS, this study introduces a surface-focused, event-based diagnostic perspective relevant to post-flashover condition assessment.

3.4. Quantitative Interpretation of Short-Term Wettability Degradation Based on Normalized Indicators

This section strictly interprets post-flashover wettability changes as surface-condition indicators relevant to moisture-driven degradation, without invoking chemical bonding, spectroscopic evidence, or bulk material transformation. These post-flashover changes are relevant to moisture-driven surface degradation because they may promote localized conductive pathways and persistent electrolyte-film formation on contaminated ceramic surfaces. Flashover events impose localized electrical and thermal stresses that disturb surface continuity, increase micro-scale defect density, and alter water–surface interaction behavior, thereby influencing moisture retention without inducing bulk material transformation [1–3,6]. These surface-level modifications govern the formation and persistence of thin electrolyte films under humid tropical environments, which are widely recognized as precursors to moisture-driven surface deterioration [4–6].

From a degradation perspective, reduced contact-angle stability indicates enhanced moisture residence time on the insulator surface. Persistent moisture films act as conductive

electrolytes, facilitating ionic transport and physicochemical surface processes that accelerate surface deterioration under humid and polluted conditions [4–6,12,32]. Consequently, wettability evolution serves as an indirect yet sensitive indicator of early-stage surface degradation linked to persistent electrolyte-film formation and moisture-assisted surface conductivity, particularly for ceramic insulation systems operating in tropical environments where moisture-assisted degradation dominates long-term performance loss [1,6,32].

The improved wettability stability observed for TiO_2-RTV and SiO_2-RTV nanocomposite coatings after flashover exposure indicates enhanced resistance to moisture-driven surface degradation. The reduced dispersion of post-flashover contact-angle values suggests a more homogeneous surface response to water interaction, suppressing localized moisture accumulation sites that typically initiate degradation progression and moisture-assisted surface damage [7–9,16,20]. This stabilization effect highlights the role of RTV-based nanocomposite coatings in maintaining surface continuity and limiting electrolyte-film formation immediately following electrical surface stress. These results should be interpreted strictly as surface-condition indicators rather than direct evidence of corrosion or bulk material degradation.

To quantitatively resolve these short-term surface-condition changes, normalized wettability indicators were employed. Relative Wettability Retention (RWR) captures the ability of the surface to preserve hydrophobicity after flashover exposure, while the Wettability Degradation Index (WDI) represents the severity of surface destabilization due to moisture interaction. As summarized in Table 1, the uncoated ceramic surface exhibits the lowest RWR and the highest WDI, confirming severe surface degradation and high susceptibility to moisture-assisted deterioration. In contrast, both TiO_2-RTV and SiO_2-RTV coatings maintain higher RWR values and lower WDI values, indicating improved post-flashover surface stability. Among them, the SiO_2-RTV coating exhibits the most favorable normalized performance, which is consistent with its superior contact-angle stability and more uniform surface response after flashover exposure.

Table 1. Quantitative wettability-retention metrics derived from contact-angle measurements before and after flashover exposure.

Sample	CA_Before (°)	CA_After (°)	RWR (%)	WDI
Uncoated	42.6	18.3	43.0	0.57
TiO_2-RTV	112.4	86.7	77.1	0.23
SiO_2-RTV	115.8	92.6	80.0	0.20

Importantly, the present interpretation is strictly based on surface-condition diagnostics derived from wettability behavior and qualitative surface morphology observations, without invoking chemical bonding analysis, spectroscopic interpretation, or bulk compositional changes. By adopting an event-based, surface-focused diagnostic framework, this study provides a practical methodology for evaluating early-stage degradation mechanisms without reliance on long-term aging tests as the primary assessment approach. The normalized wettability indicators therefore offer a simple but effective quantitative basis for comparing coating effectiveness under short-term flashover-induced surface stress in humid outdoor environments.

Relative Wettability Retention (RWR, %):

$$RWR = \frac{CA_{after}}{CA_{before}} \times 100 \quad (1)$$

Wettability Degradation Index (WDI):

$$WDI = 1 - \frac{CA_{after}}{CA_{before}} \quad (2)$$

3.5. Extended Experimental Validation Using Flashover and Leakage-Current Measurements

To further support the surface-condition evaluation, supplementary flashover-voltage and leakage-current measurements were considered under controlled wet and dry conditions. These additional electrical results were not intended to replace the primary surface-based framework of the study, but rather to provide limited supporting evidence for comparison with the wettability- and morphology-based observations discussed in previous sections [1–3,20,35–37]. The summarized results are presented in Tables 2 and 3.

Table 2. Flashover voltage and leakage current measured at 50% of flashover voltage under wet conditions.

Sample	Flashover Voltage (kV)	Leakage Current at 50% of Flashover Voltage (mA)
Uncoated	37	0.016
TiO_2-RTV	38	0.016
SiO_2-RTV	35	0.016

Table 3. Flashover voltage measured under dry conditions.

Sample	Flashover Voltage (kV) Mean ± SD (n = 6)
Uncoated	15.33 ± 2.58
TiO_2-RTV	17.67 ± 2.07
SiO_2-RTV	17.92 ± 2.06

As shown in Table 2, the wet-condition flashover-voltage measurements indicate only limited electrical separation among the uncoated and coated samples under the investigated conditions. Although the TiO_2-RTV-coated sample shows a slightly higher flashover-voltage value than the uncoated ceramic, the overall variation remains small, and the SiO_2-RTV-coated sample does not exhibit a higher flashover-voltage value than the uncoated condition. In addition, the recorded leakage-current values at 50% of flashover voltage are identical for all tested samples. Accordingly, these supplementary wet-condition electrical results should be interpreted cautiously and should not be taken as the dominant basis for performance ranking among the coating systems. Under the present wet-condition measurements, the electrical data mainly indicate that the differences among the tested surfaces remain limited at this stage of evaluation [20].

The dry-condition results summarized in Table 3 also show a relatively narrow variation in flashover response among the tested samples. The flashover-voltage values remain within a close range, indicating that the application of TiO_2-RTV and SiO_2-RTV coatings does not fundamentally change the intrinsic dielectric breakdown threshold of the ceramic substrate under dry conditions. These observations are consistent with the interpretation that the principal role of the RTV-based nanocomposite coatings is associated more strongly with surface-related moisture behavior than with substantial modification of the intrinsic bulk electrical strength of the ceramic body [8–10,20,35,36].

Overall, the supplementary electrical results remain broadly consistent with the contact-angle-based and morphology-based interpretation presented in this study. Although the electrical separation among samples is limited under the present wet-condition measurements, the results still support the interpretation that the main contribution of the

RTV-based nanocomposite coatings lies in improving surface moisture behavior rather than fundamentally changing the intrinsic dielectric strength of the ceramic body [4–7,16,20].

3.6. Integrated Interpretation of Short-Term Surface Stability After Flashover Pre-Stress

The combined experimental evidence obtained from surface morphology observations (Section 3.2), static contact-angle measurements (Section 3.3), and normalized wettability indicators (Section 3.4) enables an integrated interpretation of short-term surface stability following flashover pre-stress. Rather than treating wettability degradation as an isolated parameter, the present results demonstrate that flashover-induced surface response is governed by the ability of the surface to maintain morphological continuity and suppress rapid moisture spreading immediately after electrical stressing, as reported in previous studies on electrically stressed ceramic insulators and RTV-coated systems [1–3].

For the uncoated ceramic insulator, the convergence of SEM observations, contact-angle reduction, and extreme normalized degradation indices indicates a coherent degradation pathway. The presence of open pores and microcracks observed after flashover (Section 3.2) directly corresponds to a sharp decrease in contact angle (Figure 7) and the lowest RWR combined with the highest WDI (Table 1). This consistency confirms that flashover exposure rapidly transforms the surface into a moisture-favorable state, leading to irreversible loss of short-term wettability resistance under humid conditions, in agreement with earlier investigations on untreated ceramic insulators subjected to electrical and environmental stress [3–5].

In contrast, RTV-based nanocomposite coatings fundamentally modify this surface-response trajectory. Despite exposure to identical flashover pre-stress, both TiO_2-RTV and SiO_2-RTV coatings maintain substantially higher post-flashover contact angles and exhibit significantly lower degradation severity as quantified by RWR and WDI. This behavior indicates that nanocomposite coatings do not merely delay wetting but actively stabilize the post-flashover surface condition by preserving surface continuity and limiting the formation of moisture-conductive pathways, consistent with the hydrophobic stabilization mechanisms reported for RTV-based coatings [6–8].

A key experimental distinction emerges between the two nanocomposite systems. While both coatings provide effective short-term protection, the SiO_2-RTV coating consistently demonstrates superior surface stability across all evaluation metrics. Its higher RWR and lower WDI values, together with smoother post-flashover morphology, indicate that silica-reinforced RTV coatings offer enhanced resistance to flashover-induced surface destabilization. Importantly, this distinction is observable immediately after a single flashover event, highlighting the sensitivity of the adopted experimental framework to early-stage surface degradation phenomena, which are often obscured in long-term aging studies [7–9].

The novelty of this study lies in establishing an event-based, surface-condition-oriented assessment framework for ceramic insulators subjected to flashover stress. Unlike conventional studies that emphasize long-term aging, pollution accumulation, or electrical endurance testing, the present work demonstrates that short-term surface stability can be quantitatively resolved using normalized wettability indices directly linked to experimentally observed morphology. This approach enables rapid discrimination between coating formulations based on their immediate post-flashover surface response, providing a practical and reproducible methodology for evaluating coating effectiveness under humid tropical conditions [1,2,6].

By integrating morphological evidence with normalized wettability metrics, this study advances a surface-focused experimental paradigm that bridges the gap between qualitative surface observation and quantitative degradation assessment. The results confirm that

early-stage surface-condition integrity following flashover exposure is a critical determinant of wettability behavior and can be effectively captured using the proposed methodology.

4. Conclusions

This study demonstrates that TiO_2-RTV and SiO_2-RTV nanocomposite coatings significantly improve the short-term surface wettability retention of 150 kV ceramic insulators following a single flashover pre-stress under humid tropical conditions. By integrating static contact-angle measurements, qualitative surface morphology, and normalized wettability indicators, including relative wettability retention (RWR) and the wettability degradation index (WDI), an event-based framework was established to quantitatively evaluate early-stage flashover-induced surface-condition degradation.

Among the tested coating systems, the SiO_2-RTV coating exhibited the most stable post-flashover wettability retention, indicating superior resistance to moisture-assisted surface degradation under the investigated conditions. The supplementary flashover-voltage and leakage-current results were consistent with the wettability- and morphology-based interpretation, confirming that the primary contribution of the RTV-based nanocomposite coatings lies in improving surface moisture behavior and suppressing conductive film continuity, rather than fundamentally altering the intrinsic dielectric strength of the ceramic substrate.

Overall, the findings support the use of nanoparticle-modified RTV coatings, particularly SiO_2-RTV, as promising candidates for rapid post-event surface-performance screening of ceramic insulators in humid outdoor service environments. The proposed surface-focused, event-based framework provides a practical experimental basis for evaluating short-term degradation behavior associated with flashover-induced surface-condition changes, without requiring long-term aging experiments as the primary assessment approach. This study focuses on early-stage surface-condition changes associated with flashover-induced wettability response and does not directly investigate corrosion processes. Because the experiments were performed on a controlled $n = 3$ dataset per group, the present results should be interpreted as comparative laboratory evidence and should be further validated in larger-scale studies.

Author Contributions: Conceptualization, Y.W. and S.S.; methodology, Y.W. and N.H.; validation, S.A., A.S.W., and A.M.N.P.; formal analysis, H.H. and M.M.; investigation, M.N.N.; writing—original draft, Y.W.; writing—review and editing, S.S. and all authors. All authors have read and agreed to the published version of the manuscript.

Funding: This research was financially supported by the National Research and Innovation Agency of Indonesia (BRIN) under Research Grant Agreements No. 15/IV/KS/02/2025 and No. 25/27.O10.1.2/PN/IV/2025.

Data Availability Statement: The data supporting the findings of this study are available from the corresponding author upon reasonable request. The experimental data, including raw contact-angle measurements, coating compositions, and image analyses, were obtained from laboratory experiments conducted at Institut Teknologi Padang (ITP), Universitas Andalas (UNAND), and the National Research and Innovation Agency of Indonesia (BRIN).

Acknowledgments: The authors also acknowledge the technical support and laboratory facilities provided by Institut Teknologi Padang (ITP), Universitas Andalas (UNAND), and the National Research and Innovation Agency of Indonesia (BRIN) during the experimental work, including FTIR, SEM, and FESEM characterization as well as flashover and leakage-current testing.

Conflicts of Interest: The authors declare no conflicts of interest.

Appendix A. Representative Raw Contact-Angle Measurement Images

Representative raw contact-angle screenshots obtained during goniometer acquisition are provided in this appendix to directly address Reviewer 3′s request for measurement images. Each screenshot shows the droplet profile, software-based baseline fitting, and left/right angle detection used to calculate the reported average contact angle values. The appendix presents representative examples from different sample conditions and measurement points.

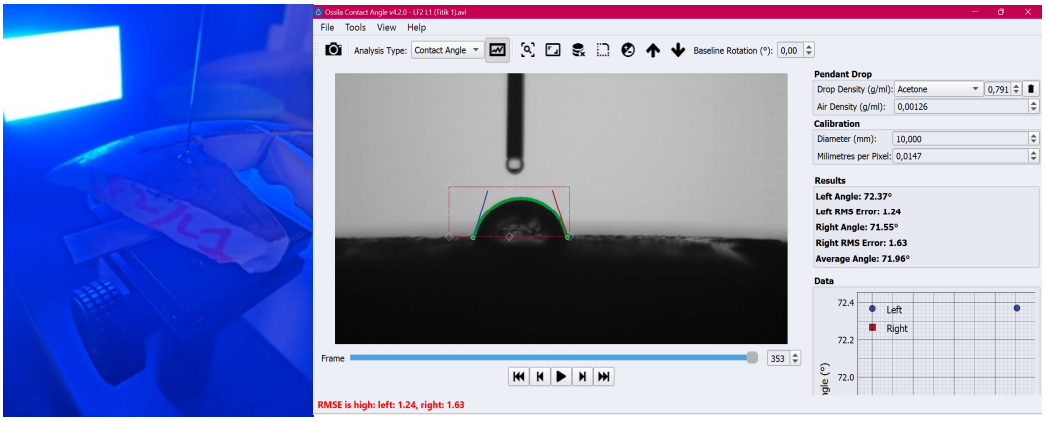


Figure A1. Representative raw contact-angle measurement images of the uncoated sample at point-1.

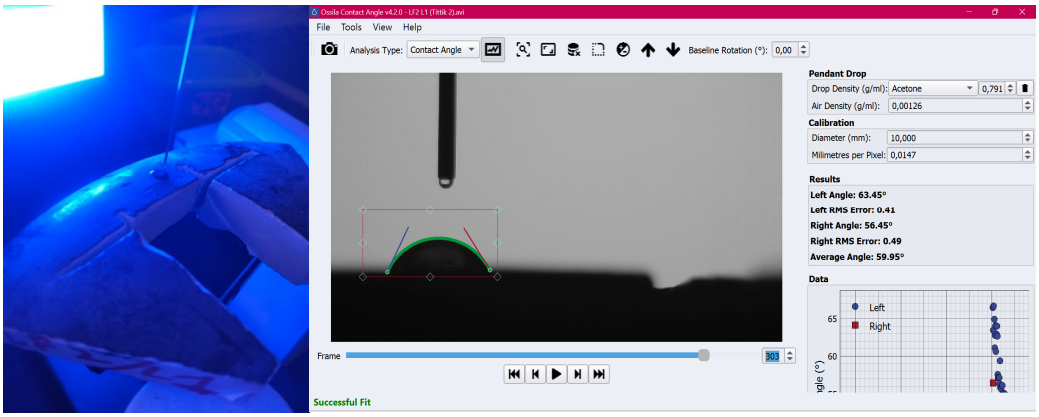


Figure A2. Representative raw contact-angle measurement images of the uncoated sample at point-2.

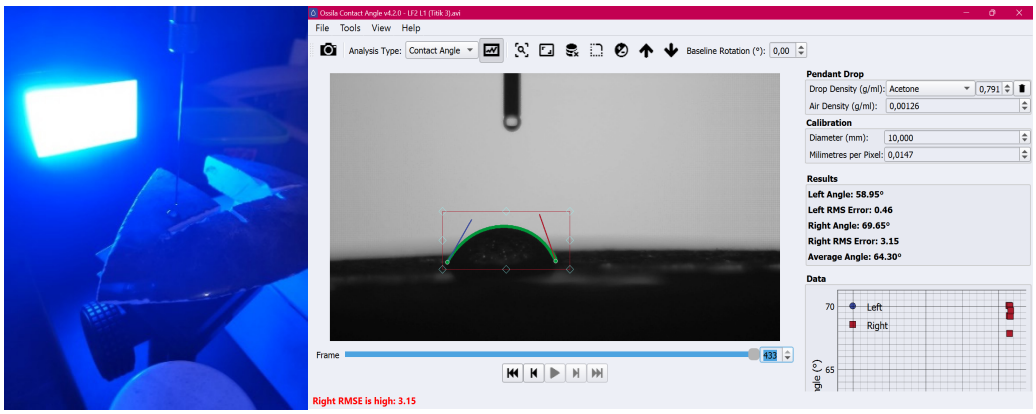


Figure A3. Representative raw contact-angle measurement images of the uncoated sample at point-3.

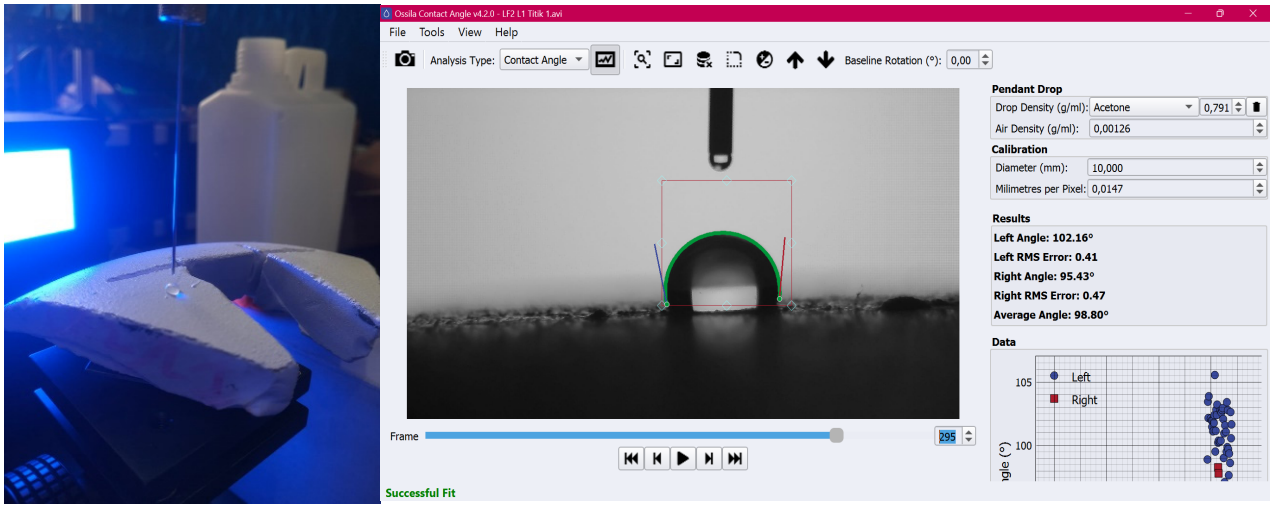


Figure A4. Representative raw contact-angle measurement images of the TiO_2-RTV-coated sample at point-1.

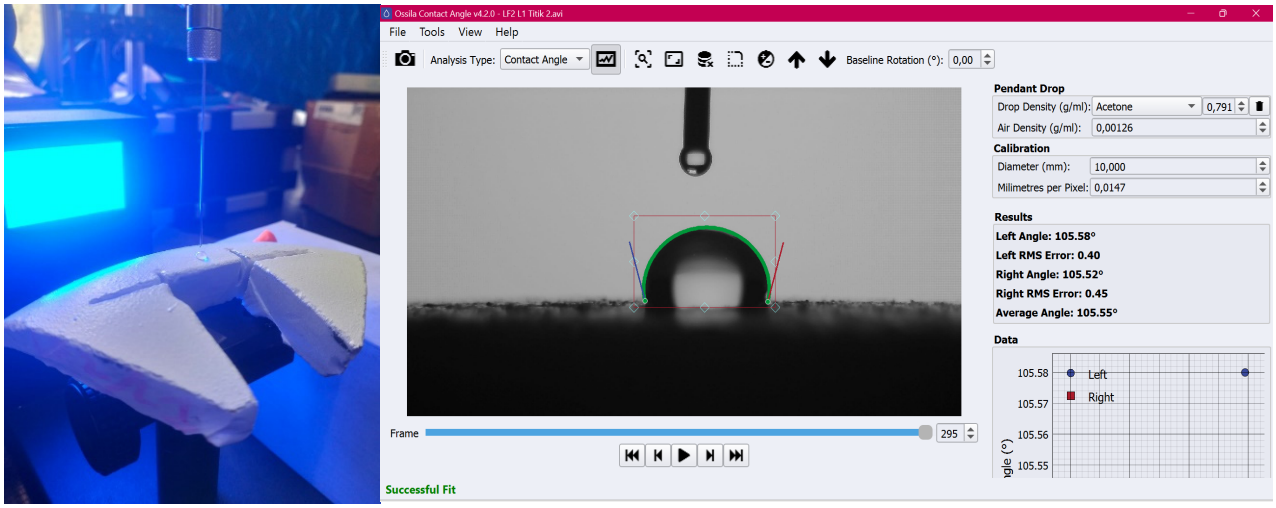


Figure A5. Representative raw contact-angle measurement images of the SiO_2-RTV-coated sample at point-2.

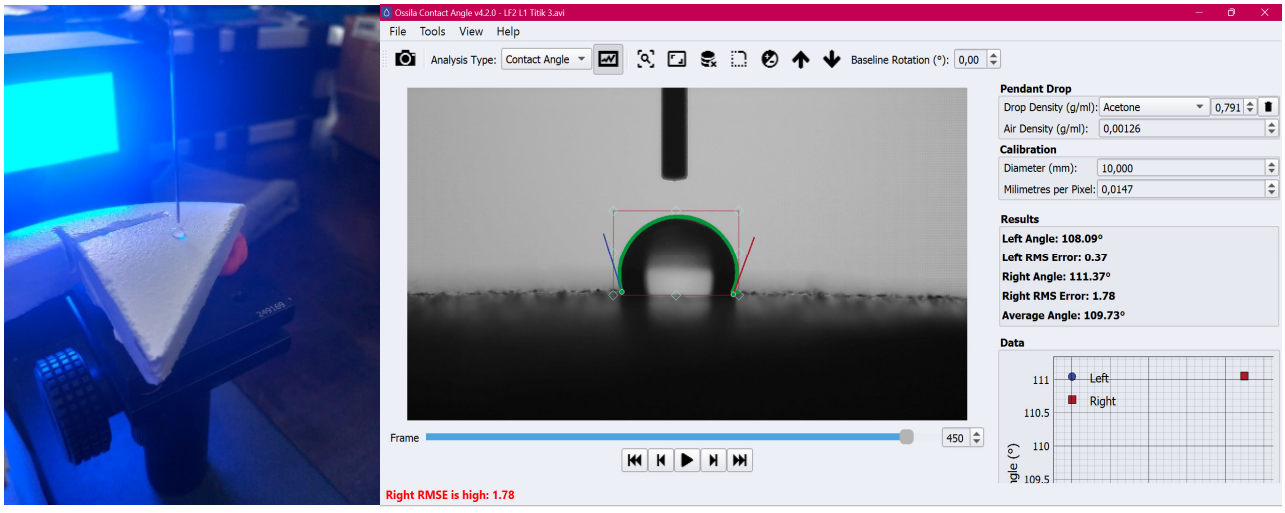


Figure A6. Representative raw contact-angle measurement images of the SiO_2-RTV-coated sample at point-3.

References

1. Ouchen, L.; Bayadi, A.; Boudissa, R. Dynamic model to predict the characteristics of the electric arc around a polluted insulator. *IET Sci. Meas. Technol.* **2020**, *14*, 83–90. [CrossRef]
2. Warmi, Y.; Zulkarnaini; Rajab, A.; Yuanisa, C.; Elyas, R.O.; Putra, A.M.N.; Anthony, Z. An optimal design of grounding system for tower footings in Payakumbuh 150 kV transmission line of Koto Panjang. *Int. J. Adv. Sci. Eng. Inf. Technol.* **2023**, *13*, 844–850. [CrossRef]
3. Hu, Q.; Li, Q.; Liu, Z.; Xue, N.; Ren, H.; Haddad, M. Surface flashover induced by metal contaminants adhered to tri-post epoxy insulators under superimposed direct and lightning impulse voltages. *Polymers* **2022**, *14*, 1374. [CrossRef] [PubMed]
4. Qin, X.; Zhang, F.; Chen, S.; Wang, T.; Hong, X.; Wang, X.; Jia, Z. Characterization of hygroscopic insulator contamination via laser-induced breakdown spectroscopy. *IEEE Trans. Plasma Sci.* **2021**, *49*, 1166–1172. [CrossRef]
5. Cao, B.; Shen, S.; Li, Z.; Yang, D.; Wang, L. Insulator contamination monitoring based on its hygroscopicity under unsaturated humidity. *IEEE Trans. Instrum. Meas.* **2022**, *71*, 1–8. [CrossRef]
6. Manjang, S.; Syafaruddin; Tambi; Musaruddin, M.; Kitta, I. Study of leakage current characteristics of high-voltage insulators ageing after dry season in polluted environmental conditions. In Proceedings of the 2021 International Conference on High Voltage Engineering and Power Systems (ICHVEPS), Bandung, Indonesia, 5–6 October 2021; pp. 74–78. [CrossRef]
7. Al-Karawi, S.; Al-Taie, A. Superhydrophobic coating for enhancing porcelain insulator performance under pollution conditions. *e-Prime Adv. Electr. Eng. Electron. Energy* **2024**, *8*, 100515. [CrossRef]
8. Suwarno; Pratomosiwi, F. Application of RTV silicone rubber coating for improving performances of ceramic outdoor insulator under polluted condition. In Proceedings of the 2009 International Conference on Electrical Engineering and Informatics (ICEEI), Selangor, Malaysia, 5–7 August 2009; pp. 581–587. [CrossRef]
9. Ouyang, X.; Yin, F.; Jia, Z.; Yang, S.; Wang, Y.; Bai, H.; Zhang, X.; Li, Y.; Chen, H. Research of biological contamination and its effect on the properties of RTV-coated insulators. *Electr. Power Syst. Res.* **2019**, *167*, 138–149. [CrossRef]
10. Olad, A.; Maryami, F.; Mirmohseni, A.; Shayegani-Akmal, A.A. Potential of SLIPS coatings as flashover inhibitors on porcelain insulators in icing, contaminated, and harsh environments. *Prog. Org. Coat.* **2021**, *151*, 106082. [CrossRef]
11. Liu, Y.; Guo, Y.; Wang, B.; Zhang, X.; Huang, G.; Zhang, G.; Liu, Y.; Deng, Q.; Wu, G. Pollution morphology characteristics on a superhydrophobic surface and its pollution flashover voltage in DC electric field. *High Volt.* **2022**, *7*, 564–574. [CrossRef]
12. Salem, A.A.; Al-Gailani, S.A.; Amer, A.A.G.; Alsharef, M.; Bajaj, M.; Zaitsev, I.; Ngah, R.; Ghoneim, S.S.M. Classification of RTV-coated porcelain insulator condition under different profiles and levels of pollution. *Sci. Rep.* **2024**, *14*, 22759, Erratum in *Sci. Rep.* **2025**, *15*, 3935. [CrossRef]
13. Taghvaei, M.; Sedighizadeh, M.; NayebPashaee, N.; Fini, A.S. Reliability assessment of RTV and nano-RTV-coated insulators concerning contamination severity. *Electr. Power Syst. Res.* **2021**, *191*, 106892. [CrossRef]
14. Suwarno; Basuki, A.; Lendy, F.; Sumedi. Improving outdoor insulator performance installed at coastal area using silicone rubber coating. In Proceedings of the 2012 International Conference on Condition Monitoring and Diagnosis (CMD), Bali, Indonesia, 23–27 September 2012; pp. 1143–1146. [CrossRef]
15. Li, Y.; Song, Z.; Tian, Y.; Yang, C.; Liu, F.; Bai, H.; Zhao, F.; Liu, X.; Yang, H. Study on the algae contamination and its effects on the properties of RTV-coated insulators. *Energies* **2022**, *15*, 5216. [CrossRef]
16. Zolriasatein, A.; RajabiMashhadi, Z.; Rezaei Abadchi, M.; Riahi Noori, N.; Abyazi, S. A new approach based on RTV/SiO_2 nano coating to tackling environmental pollution on electrical energy distributions. *J. Renew. Energy Environ.* **2022**, *9*, 45–51. [CrossRef]
17. Esfarjani, A.; Shokrieh, M.M. Effects of TiO_2 nanoparticles and silane coupling agents on the adhesion strength and weathering properties of silicone rubber coatings. *Int. J. Adhes. Adhes.* **2024**, *130*, 103604. [CrossRef]
18. Isa, M.; Othman, M.; Abdullah, A.Z.; Piah, M.A.M.; Rahman, N.A.; Mazlee, M.N. Characteristics of RTV coating on ceramic insulator. In Proceedings of the 2019 IEEE International Conference on Automatic Control and Intelligent Systems (I2CACIS), Selangor, Malaysia, 29 June 2019; pp. 114–117. [CrossRef]
19. Li, Z.; Yin, F.; Cao, B.; Wang, L.; Shao, S.; Farzaneh, M. Pollution flashover performance of RTV coatings with partial damage. *Int. J. Electr. Power Energy Syst.* **2020**, *121*, 106102. [CrossRef]
20. Zhang, Z.; Qiao, X.; Xiang, Y.; Jiang, X. Comparison of surface pollution flashover characteristics of RTV-coated insulators under different coating damage modes. *IEEE Access* **2019**, *7*, 40904–40912. [CrossRef]
21. Ullah, I.; Akbar, M.; Khan, H.A. Enhancement of electrical, mechanical and thermal properties of silicone-based coating with alumina-trihydrate/silica for ceramic insulators. *Mater. Chem. Phys.* **2022**, *282*, 125972. [CrossRef]
22. Shajari-Ghasemkheili, S.; Sarraf-Mamoory, R. Development of a transparent silica-titania-methyl siliconate nanocoating with photocatalytic-hydrophobic properties aided by response surface method. *Mater. Res. Express* **2019**, *6*, 106430. [CrossRef]
23. Pal, A.K.; Baral, A.; Lahiri, A. Studies on prospect of HTV silicone rubber as dielectric material when reinforced with TiO_2 nanoparticles. *IET Sci. Meas. Technol.* **2021**, *15*, 292–301. [CrossRef]
24. Salem, A.A.; Abd-Elhady, A.M.; Balbaa, M.A.; El-Zein, A. Pollution flashover characteristics of coated insulators under different profiles of coating damage. *Coatings* **2021**, *11*, 1194. [CrossRef]

25. Khatoon, S.; Khan, A.A.; Tariq, M.; Alamri, B.; Mihet-Popa, L. Flashover voltage prediction models under agricultural and biological contaminant conditions on insulators. *Energies* **2022**, *15*, 1297. [CrossRef]
26. Yang, S.; Jia, Z.; Ouyang, X. Effects of asymmetrical algal distribution on the AC flashover characteristics of bio-contaminated silicone rubber insulators. *Electr. Power Syst. Res.* **2019**, *172*, 296–302. [CrossRef]
27. Dolník, B.; Sarpataky, L.; Bucko, S.; Pavlík, M.; Stefko, R. Assessing contamination severity of high-voltage insulators using dielectric loss factor: Laboratory measurements and comparative analysis of leakage current and dielectric loss factor at different voltage levels, humidity, and insulating materials. *Electr. Power Syst. Res.* **2023**, *225*, 109855. [CrossRef]
28. Savadkoohi, E.M.; Mirzaie, M.; Seyyedbarzegar, S.M.; Mohammadi, M.; Khodsuz, M.; Pashakolae, M.G.; Ghadikolaei, M.B. Experimental investigation on composite insulators AC flashover performance with fan-shaped non-uniform pollution under electro-thermal stress. *Int. J. Electr. Power Energy Syst.* **2020**, *121*, 106142. [CrossRef]
29. Karaman, H.S.; Sherif, S.M.M.; El-Gamal, S.M.A.; Abdel-Rahim, N.; Abd-Allah, M.A. Performance enhancing of porcelain insulators using low-cost micro additives. *Ain Shams Eng. J.* **2024**, *15*, 102622. [CrossRef]
30. Mahdjoubi, A.; Zegnini, B.; Belkheiri, M.; Seghier, T. Fixed least squares support vector machines for flashover modelling of outdoor insulators. *Electr. Power Syst. Res.* **2019**, *173*, 29–37. [CrossRef]
31. Deb, S.; Das, S.; Pradhan, A.K.; Banik, A.; Chatterjee, B.; Dalai, S. Estimation of contamination level of overhead insulators based on surface leakage current employing detrended fluctuation analysis. *IEEE Trans. Ind. Electron.* **2020**, *67*, 5729–5736. [CrossRef]
32. Sit, K.; Das, A.K.; Mukherjee, D.; Haque, N.; Deb, S.; Pradhan, A.K.; Dalai, S.; Chatterjee, B. Condition monitoring of overhead polymeric insulators employing hyperbolic window Stockwell transform of surface leakage current signals. *IEEE Sens. J.* **2021**, *21*, 10957–10964. [CrossRef]
33. Seyedmehdi, S.A.; Zhang, H.; Zhu, J. Superhydrophobic RTV silicone rubber insulator coatings. *Appl. Surf. Sci.* **2012**, *258*, 2972–2976. [CrossRef]
34. Amalia, S.; Rajab, A.; Novizon, N.; Warmi, Y.; Kasmar, A.F. The effect of humidity and temperature on flashover in high-voltage transmission-line ceramic insulators. *TEM J.* **2024**, *13*, 670–680. [CrossRef]
35. Warmi, Y.; Amalia, S.; Zulkarnaini; Dasman; Bachtiar, A.; Anthony, Z.; Azhar, H. Modeling and simulation for flashover location determination on 150 kV insulator string. *Int. J. Electr. Comput. Eng.* **2024**, *14*, 3716–3728. [CrossRef]
36. Amalia, S.; Rajab, A.; Novizon; Warmi, Y.; Kasmar, A.F. Investigation of leakage current in 150 kV Payakumbuh–Koto Panjang insulators. *J. Phys. Conf. Ser.* **2024**, *2923*, 012011. [CrossRef]
37. Zhu, Y.; Zhou, R.; Zhang, Y.; Dong, X.; Huang, X. Review on flashover risk prediction method of iced insulator based on icing monitoring technology. *Cold Reg. Sci. Technol.* **2021**, *185*, 103252. [CrossRef]

Disclaimer/Publisher's Note: The statements, opinions and data contained in all publications are solely those of the individual author(s) and contributor(s) and not of MDPI and/or the editor(s). MDPI and/or the editor(s) disclaim responsibility for any injury to people or property resulting from any ideas, methods, instructions or products referred to in the content.